

Energy difference between the lowest doublet and quartet states of the boron atomKrzysztof Strasburger *Department of Physical and Quantum Chemistry, Faculty of Chemistry, Wrocław University of Science and Technology, Wybrzeże Wyspiańskiego 27, PL-50-370 Wrocław, Poland*

(Received 21 September 2020; accepted 14 October 2020; published 9 November 2020)

The energies of the lowest 2P_u , 4P_g , and $2D_g$ states of the boron atom are calculated with μ hartree accuracy, in the basis of symmetrized, explicitly correlated Gaussian lobe functions. Finite nuclear mass and scalar relativistic corrections are taken into account. This study contributes to the problem of the energy differences between doublet and quartet states of boron, which have not been measured to date. It is found that the ${}^2P_u \rightarrow {}^4P_g$ excitation energy, recommended in the Atomic Spectra Database, appears underestimated by more than 300 cm^{-1} .

DOI: [10.1103/PhysRevA.102.052806](https://doi.org/10.1103/PhysRevA.102.052806)**I. INTRODUCTION**

Highly accurate calculations, carried out within the well-grounded theory of quantum mechanics, are currently possible for few-electron atoms and molecules. The results are usually compared with spectroscopic data. This collation verifies the theory and computational methods, but may also stimulate improvements of the experiment. History of the studies on the rovibrational spectrum of the hydrogen molecule is a good example of such positive feedback [1,2]. The calculations may also provide reliable results where experimental data are missing. For the boron atom, intersystem radiative transitions were not observed, therefore the energy differences between the spin doublet and quartet states, listed in the Atomic Spectra Database (ASD) [3] are based on numerical extrapolation of the transition energies known for heavier, isoelectronic ions [4].

According to this extrapolation, the lowest 4P_g term has the energy higher by $28\,644.3\text{ cm}^{-1}$, than the ground state term (2P_u). The J quantum number is omitted, because the fine structure is not considered in the present work. The energy of a nonsplit term is not observable, and is computed from experimental data, as weighted average over associated, J -dependent term energies. Calculations of this energy difference were also carried out in the past, but the results do not agree with that “experimental” value. The short review is limited to most recent articles, because the results of earlier calculations [5,6] were simply too inaccurate for a comparison with spectroscopic data. Froese Fischer and coworkers [7] used the multiconfiguration Hartree-Fock (MCHF) method, with finite nuclear mass and scalar relativistic corrections taken into account, and obtained the excitation energy amounting to $28\,959(5)\text{ cm}^{-1}$. It is to be noted that their computational method was validated for the carbon cation, with theoretical result different from experimental one by only 7 cm^{-1} . Chen [8] predicted $28\,719.46\text{ cm}^{-1}$, using configuration interaction wave function, and also including relativistic and finite nuclear mass corrections. Nakatsuji

and coworkers [9] employed the free-complement chemical-formula-theory (FC-CFT) method. The value of $28\,826\text{ cm}^{-1}$ is obtained, with their nonrelativistic, fixed-nucleus energies, and assuming that the respective corrections would contribute c.a. 50 cm^{-1} , similarly as in the calculations by Chen and Froese Fischer. The largest discrepancy between theoretical and experimental excitation energy exceeds 300 cm^{-1} . Computational results are, however, rather scattered and a decisive calculation requires a wave function that provides sufficiently accurate absolute electronic energies. Apart of the 2P_u and 4P_g states, the lowest 2D_g state is also the subject of the present study, because the transition energies to the latter, from the ground state, are known and may serve for the estimation of uncertainty of final results. The experiment-based energy difference between 2P_u and 2D_g terms amounts to $47\,846.74\text{ cm}^{-1}$ [3].

In theoretical studies of the boron atom, not necessarily aimed at the ${}^2P_u \rightarrow {}^4P_g$ excitation, most efforts to date were devoted to the ground state [10–12]. Preliminary Hylleraas-CI calculations were reported by Ruiz [13]. Highly accurate, nonrelativistic energies were obtained with the explicitly correlated r_{12} -MR-CI method [14], and in the diffusion Monte Carlo (DMC) simulations [15]. There is a masterpiece of CI calculations, by Almora-Diaz and Bunge [16], with the orbital basis containing functions corresponding to the l quantum number reaching 20 (z -type orbitals), yielding the energy only $31\ \mu$ hartree above the variational limit. Well-hit extrapolation to the complete basis set missed this limit by $6\ \mu$ hartree. Best results were obtained with explicitly correlated Gaussian functions (ECG) [17,18]. The estimated error of nonrelativistic energy of this state was smaller than $1\ \mu$ hartree. Similar accuracy was achieved for the 2S_g states, and the transition energies between the ground state and S -symmetry states were reproduced within a fraction of cm^{-1} , with finite nuclear mass, relativistic (including fine and hyperfine structure for the ground-state term) and leading radiative corrections taken into account.

The wave functions and energies of comparable accuracy are missing for the 4P_g and 2D_g states, and the results are scarce in the literature [5–7,9]. The present paper is aimed at filling in this hole, and contributing to final resolution of the discrepancies concerning the energy differences between the spin doublet and quartet terms of the boron atom.

Nonrelativistic wave functions, expressed as linear combinations of symmetry-adapted, explicitly correlated Gaussian functions, and variational energies with scalar relativistic corrections are obtained for the lowest 2P_u , 4P_g , and 2D_g states. Atomic units are used unless stated otherwise. The conversion factor to the energy unit used commonly in spectroscopy amounts to 1 hartree=219 474.63 cm⁻¹

II. METHOD

The stationary Schrödinger equation for the n -electron atom is solved with the nonrelativistic Hamiltonian,

$$\hat{H} = -\frac{\nabla_{\text{nuc}}^2}{2m_{\text{nuc}}} + \sum_{i=1}^n \left(-\frac{\nabla_i^2}{2} - \frac{Z}{r_i} \right) + \sum_{i>j=1}^n \frac{1}{r_{ij}}, \quad (1)$$

where i and j count the electrons. Details of the method have been introduced in earlier papers devoted to the lithium and carbon atoms [19,20], and various states of many-electron harmonium [21–24]. The wave function,

$$\begin{aligned} \Psi(\mathbf{r}_1, s_1, \dots, \mathbf{r}_n, s_n) \\ = \sum_{I=1}^K C_I \hat{A} \Theta_I(s_1, \dots, s_n) \hat{P} \chi_I(\mathbf{r}_1, \dots, \mathbf{r}_n), \end{aligned} \quad (2)$$

is expressed as a linear combination of explicitly correlated Gaussian primitives (lobes),

$$\chi_I(\mathbf{r}_1, \dots, \mathbf{r}_n) = \exp \left[-\sum_{i=1}^n a_{I,i} (\mathbf{r}_i - \mathbf{R}_{I,i})^2 - \sum_{i>j=1}^n b_{I,ij} r_{ij}^2 \right], \quad (3)$$

symmetrized by the spatial symmetry projector \hat{P} , proper for chosen one-dimensional, irreducible representation of the selected finite point group. This wave function is not an eigenfunction of the square of the angular momentum operator (\hat{L}^2), for nonzero $\mathbf{R}_{I,i}$ vectors. The deviation from the exact $L(L+1)$ eigenvalue is effectively diminished by the procedure of variational energy minimization, in which the parameters (linear C_I and nonlinear $a_{I,i}$, $b_{I,ij}$, and $\mathbf{R}_{I,i}$) are established. Action of \hat{P} upon χ_I annihilates from the wave function, a finite subset of unwanted components, whose symmetry properties are specific to some other representations of the K_h point group, and ensures convergence towards the desired state. $\Theta_I(s_1, \dots, s_n)$ is the spin function, common for all basis functions for a given state, which is sufficient, because the spatial functions are nonorthogonal. Namely,

$$\begin{aligned} \Theta_I(s_1, \dots, s_5) = [\alpha(1)\beta(2) - \beta(1)\alpha(2)] \\ \times [\alpha(3)\beta(4) - \beta(3)\alpha(4)]\alpha(5) \end{aligned} \quad (4)$$

is used for both doublets, and

$$\Theta_I(s_1, \dots, s_5) = [\alpha(1)\beta(2) - \beta(1)\alpha(2)]\alpha(3)\alpha(4)\alpha(5) \quad (5)$$

for the quartet. \hat{A} is the antisymmetrizer, which ensures proper permutational symmetry of the wave function.

The relativistic energy of a resting system may be written as the power series of the fine structure constant $\alpha = \frac{1}{4\pi\epsilon_0} \frac{e^2}{\hbar c}$. Omitting the rest mass contribution,

$$E_{\text{rel}} = E_{nr} + E^{(2)} + E^{(3)} + \dots, \quad (6)$$

where E_{nr} is the nonrelativistic energy, $E^{(2)}$ contains the Breit-Pauli relativistic corrections, and higher order terms are known as the radiative (QED) corrections. All these corrections may be calculated in a perturbative manner, as expectation values of respective operators, with a known nonrelativistic wave function. The Breit-Pauli Hamiltonian may be split to the relativistic shift \hat{H}_{RS} operator, with the expectation value E_{RS} , and the fine and hyperfine structure operators, which contain spin-orbit and spin-spin coupling terms. Only the former is considered in this work. It is convenient to write it down as the sum of the following terms:

$$\hat{H}_{\text{RS}} = \hat{H}_1 + \hat{H}_{1n} + \hat{H}_2 + \hat{H}_3 + \hat{H}_4 + \hat{H}_{4n}. \quad (7)$$

These operators describe, respectively, the electronic mass-velocity correction,

$$\hat{H}_1 = -\frac{1}{8c^2} \sum_{i=1}^n \nabla_i^4, \quad (8)$$

the electron-nucleus Darwin term,

$$\hat{H}_2 = \frac{Z\pi}{2c^2} \sum_{i=1}^n \delta(\mathbf{r}_i), \quad (9)$$

the sum of the electron-electron Darwin term and spin-spin Fermi contact interaction (both have the same mathematical form, after integration over spin variables [25]),

$$\hat{H}_3 = \frac{\pi}{c^2} \sum_{i>j=1}^n \delta(\mathbf{r}_{ij}), \quad (10)$$

and the electron orbit-orbit term,

$$\hat{H}_4 = \frac{1}{2c^2} \sum_{i>j=1}^n \left(\frac{\nabla_i \cdot \nabla_j}{r_{ij}} + \frac{\mathbf{r}_{ij} \cdot [(\mathbf{r}_{ij} \cdot \nabla_i) \nabla_j]}{r_{ij}^3} \right), \quad (11)$$

which describes the interaction of magnetic dipoles arising from orbital motion of the electrons. There are two terms in Eq. (7) that have nonzero value only for finite nuclear mass, namely the nuclear mass-velocity correction,

$$\hat{H}_{1n} = -\frac{1}{8m_{\text{nuc}}^3 c^2} \nabla_{\text{nuc}}^4, \quad (12)$$

and the nucleus-electron contribution to orbit-orbit magnetic interaction energy,

$$\hat{H}_{4n} = -\frac{Z}{2m_{\text{nuc}} c^2} \sum_{i=1}^n \left(\frac{\nabla_i \cdot \nabla_{\text{nuc}}}{r_{ij}} + \frac{\mathbf{r}_i \cdot [(\mathbf{r}_i \cdot \nabla_i) \nabla_{\text{nuc}}]}{r_i^3} \right). \quad (13)$$

Distinction of the cases of fixed and nonfixed nucleus requires only the modification of the nuclear mass in all

TABLE I. Nonrelativistic energies, deviations of $\langle L^2 \rangle$ from $L(L-1)$, and extrapolated energies, for fixed nucleus. For extrapolated (E_{extr}) results, standard deviations of the least significant digits are given in parentheses.

K	E_{nr}	$\langle L^2 \rangle - L(L+1)$	K	E_{nr}	$\langle L^2 \rangle - L(L+1)$
${}^2P_u (L=1)$					
277	-24.653001970	7.81×10^{-6}	2745	-24.653862346	1.73×10^{-7}
406	-24.653462344	5.76×10^{-6}	4022	-24.653865404	8.82×10^{-8}
595	-24.653681184	3.48×10^{-6}	5679	-24.653867017	4.97×10^{-8}
872	-24.653785377	1.83×10^{-6}	7456	-24.653867660	3.54×10^{-8}
1278	-24.653833991	7.33×10^{-7}	10304	-24.653868064	2.12×10^{-8}
1873	-24.653854171	3.30×10^{-7}	E_{extr}	-24.65386890(14)	0
${}^4P_g (L=1)$					
277	-24.521826756	1.10×10^{-5}	1873	-24.522039020	2.26×10^{-7}
406	-24.521944458	7.17×10^{-6}	2733	-24.522040459	1.11×10^{-7}
595	-24.521999781	3.07×10^{-6}	3580	-24.522041147	5.47×10^{-8}
872	-24.522023448	1.47×10^{-6}	4672	-24.522041430	3.49×10^{-8}
1278	-24.522035395	4.74×10^{-7}	E_{extr}	-24.52204180(5)	0
${}^2D_g (L=2)$					
277	-24.434439490	1.86×10^{-4}	2745	-24.435961389	5.34×10^{-6}
406	-24.435110865	1.43×10^{-4}	4023	-24.435972976	2.69×10^{-6}
595	-24.435568403	7.98×10^{-5}	5858	-24.435978480	1.30×10^{-6}
872	-24.435789658	4.04×10^{-5}	8231	-24.435981009	5.35×10^{-7}
1278	-24.435896508	1.90×10^{-5}	E_{extr}	-24.43598347(63)	0
1873	-24.435941219	1.01×10^{-5}			

Hamiltonians, from infinity to the one proper for a given isotope of boron. The wave function given by Eqs. (2) and (3) is expressed in relative coordinates— \mathbf{r}_i denotes the position of i^{th} electron relatively to the nucleus. Therefore explicit transformation of the operators, both nonrelativistic and relativistic, from the laboratory to the center-of-mass coordinate frame, is not necessary. Only relative coordinates appear in these operators explicitly. Each differentiation over a coordinate in the Cartesian laboratory frame, may be written as a properly weighted sum of differentiations over respective relative and center-of-mass coordinates. Differentiation of a function, which is dependent on relative coordinates only, over a center-of-mass coordinate, gives zero, so the final result is the same with nontransformed operators as with explicit elimination of the center-of-mass motion [26].

III. NUMERICAL RESULTS

In the first step, nonrelativistic wave functions are constructed. The ground-state wave function of the boron atom has P_u symmetry. Assuming the magnetic quantum number equal to 0, this symmetry is effectively represented by the A_u representation of the C_i point group, with the projector,

$$\hat{P} = \hat{E} - \hat{i}, \quad (14)$$

and all $\mathbf{R}_{l,i}$ vectors placed at the z axis of the coordinate frame. The C_{4v} point group is employed for both excited states, with $\mathbf{R}_{l,i}$ vectors confined to the xy plane. The projector proper for the A_2 representation,

$$\hat{P} = \hat{E} + \hat{C}_4^1 + \hat{C}_2 + \hat{C}_4^3 - \hat{\sigma}_{v1} - \hat{\sigma}_{v2} - \hat{\sigma}_{d1} - \hat{\sigma}_{d2}, \quad (15)$$

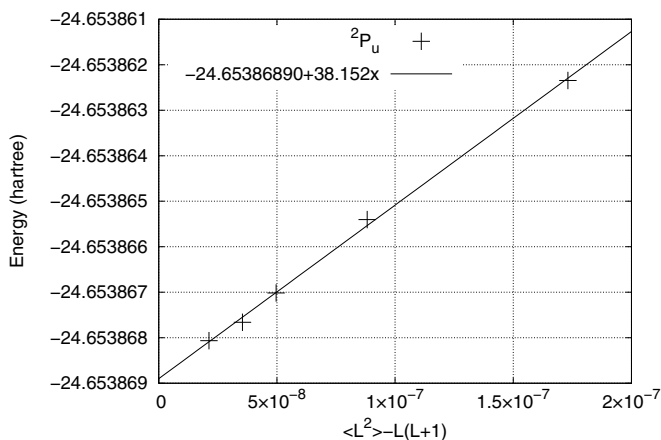


FIG. 1. Energy extrapolation using deviation of $\langle L^2 \rangle$ from $L(L+1)$, for the 2P_u state.

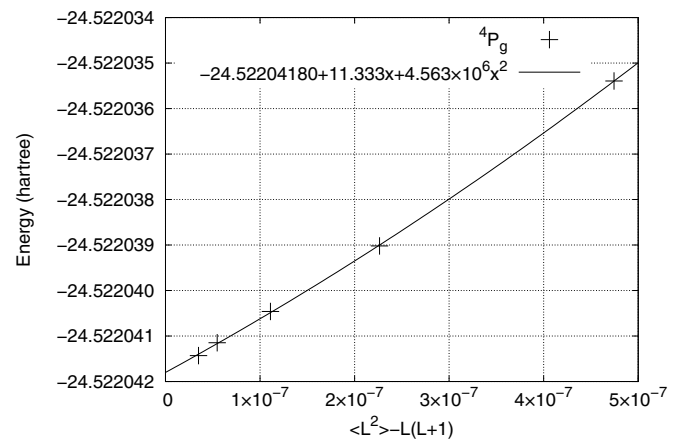


FIG. 2. Energy extrapolation using deviation of $\langle L^2 \rangle$ from $L(L+1)$, for the 4P_g state.

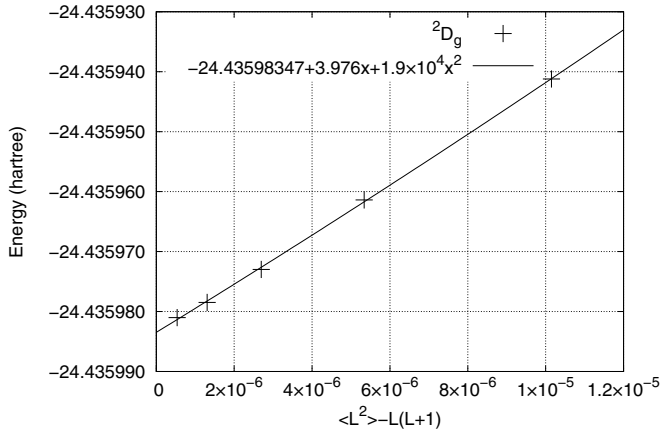


FIG. 3. Energy extrapolation using deviation of $\langle L^2 \rangle$ from $L(L+1)$, for the 2D_g state.

produces effectively the P_g symmetry of the quartet state, and the B_1 representation, with

$$\hat{P} = \hat{E} - \hat{C}_4^1 + \hat{C}_2 - \hat{C}_4^3 + \hat{\sigma}_{v1} + \hat{\sigma}_{v2} - \hat{\sigma}_{d1} - \hat{\sigma}_{d2}, \quad (16)$$

is adequate for the D_g state, producing the wave function converging to the normalized sum of eigenfunctions of \hat{L}_z , pertaining to $m_L = 2$ and $m_L = -2$.

The accuracy of nonrelativistic energies is assessed, exploiting the convergence of $\langle \hat{L}^2 \rangle$, whose known exact limits amount to $L(L+1)$. Basis sets were extended stepwise, beginning with 1, 2, and 3 ECGs and then appending functions optimized two steps back in the process, to the current set. Optimization of all variational parameters of the new basis followed, aimed at energy minimization. Successive basis sizes formed thus initially the Narayana's cows sequence [27]. For large bases, functions appeared that contributed too little to the energy, and these functions were removed from the set. The threshold value was set to 1, 0.5, or 0.2 nanohartree, dependent on the estimated distance to the variational limit. The values of nonrelativistic energies and $\langle L^2 \rangle$, calculated for infinite-mass nucleus, with K basis functions, are collected in Table I. It is noticed that the energy depends smoothly on the error of the square of angular momentum, $\langle L^2 \rangle - L(L+1)$ —

similarly as for the carbon atom [20]. This observation, which has no theoretical background and may be related to the method of construction of consecutive basis sets, gives rise to an assumption that the rotational energy error becomes nearly constant fraction of the total energy error. Either linear (for the ground state, Fig. 1) or quadratic (for both excited states, Figs. 2 and 3) functions are fitted to five best points, giving estimations of complete basis set limits of the electronic energies. Variational energies look converged to a fraction of μ hartree for 2P_u and 4P_g states, while the accuracy for the 2D_g state is a little worse, with the distance to the estimated limit still amounting to c.a. 2.5 μ hartree. The wave function of this state has apparently more complicated character, but calculation with a significantly larger basis set was not feasible.

Comparison with literature data, in Table II, reveals that the variational energy of the ground state, obtained in the present work with 7456 basis functions, is lower than the best previous result [18] by 0.5 μ hartree, and with 10 304 basis functions surpasses also the old estimate of the complete basis set limit. The $\langle L^2 \rangle$ -based extrapolation lowers this limit by 0.85 μ hartree. There are no published energies of comparable accuracies, for both excited states. The calculation by Nakatsuji [9] yielded the energy of the ground state, higher by 0.135 mhartree than the present result. On the contrary, the energy of the 4P_g state was too low, overstepping the variational limit by 0.58 mhartree. The MCHF energies by Froese Fischer [7] look more balanced, being higher by 0.345 (2P_u state) and 0.219 (4P_g state) mhartree. Most accurate non-relativistic energy of the 2D_g state, published to date [8], is by more than 2 mhartree higher than the present one.

Concerning the components of relativistic corrections (Table III), the convergence of the mass-velocity and electron-nucleus Darwin terms is still unsatisfactory for all states, with differences of few μ hartree, between the two most accurate wave functions. This inaccuracy is due to ∇^4 and $\delta(\mathbf{r})$ operators, whose expectation values converge very slowly in the basis of Gaussian functions, which do not represent properly the wave functions at coalescence points (cusps). Fortunately, the errors of $\langle \hat{H}_1 \rangle$ and $\langle \hat{H}_2 \rangle$ have opposite signs and cancel to a significant extent. The number of stable significant digits of $\langle \hat{H}_3 \rangle$ is even smaller than that of $\langle \hat{H}_2 \rangle$, but the absolute value

TABLE II. Comparison of nonrelativistic energies with published results.

Method	2P_u	4P_g	2D_g
MCHF ($l_{\max} = 7$) [5]	-24.651009		-24.431353
VMC [6]	-24.64502(6)	-24.51581(6)	-24.42486(5)
CI ($l_{\max} = 6$, selected) [8]	-24.652032	-24.521401	-24.433575
MCHF ($l_{\max} = 5$) [7]	-24.653523595	-24.521822334	
FC-CFT [9]	-24.653734(103)	-24.522622(50)	
r_{12} -MR-CI [14]	-24.653787		
DMC [15]	-24.65379(3)		
CI ($l_{\max} = 20$) [16]	-24.65383733		
CI, extrapolated [16]	-24.653862(2)		
ECG, $K=5100$ [17]	-24.65386608		
ECG, $K=8192$ [18]	-24.653867537		
ECG, extrapolated [18]	-24.65386805(45)		
ECG lobes (present work)	-24.653868064	-24.522041430	-24.435981009
E_{extr} (present work)	-24.65386890(14)	-24.52204180(5)	-24.43598347(63)

TABLE III. Scalar relativistic corrections (in mhartree), for fixed nucleus.

K	$\langle \hat{H}_1 \rangle$	$\langle \hat{H}_2 \rangle$	$\langle \hat{H}_3 \rangle$	$\langle \hat{H}_4 \rangle$	E_{RS}
2P_u					
277	-36.599999	29.743913	-0.601678	-0.057897	-7.515662
406	-36.728411	29.867256	-0.597815	-0.057872	-7.516842
595	-36.806576	29.938863	-0.595500	-0.057843	-7.521055
872	-36.834510	29.969803	-0.594004	-0.057833	-7.516544
1278	-36.863671	29.998464	-0.593480	-0.057827	-7.516515
1873	-36.873790	30.008434	-0.592950	-0.057823	-7.516129
2745	-36.893141	30.027586	-0.592638	-0.057822	-7.516015
4022	-36.897900	30.032285	-0.592543	-0.057821	-7.515980
5679	-36.904331	30.038645	-0.592389	-0.057820	-7.515896
7456	-36.910731	30.044909	-0.592249	-0.057820	-7.515891
10 304	-36.913837	30.047995	-0.592174	-0.057820	-7.515836
4P_g					
277	-36.062593	29.388974	-0.578999	-0.027932	-7.280549
406	-36.062306	29.387961	-0.576977	-0.027940	-7.279263
595	-36.120148	29.442882	-0.576059	-0.027944	-7.281270
872	-36.135572	29.460497	-0.575635	-0.027944	-7.278654
1278	-36.155086	29.479579	-0.575179	-0.027944	-7.278630
1873	-36.166969	29.491458	-0.574979	-0.027944	-7.278433
2733	-36.172481	29.496815	-0.574859	-0.027943	-7.278469
3580	-36.179044	29.503374	-0.574758	-0.027943	-7.278371
4672	-36.181062	29.505364	-0.574684	-0.027943	-7.278325
2D_g					
277	-35.970107	29.276227	-0.585496	-0.042998	-7.322373
406	-36.038120	29.340083	-0.583894	-0.043104	-7.325035
595	-36.141397	29.439580	-0.582434	-0.043201	-7.327453
872	-36.182799	29.478829	-0.581222	-0.043269	-7.328461
1278	-36.222970	29.517760	-0.580282	-0.043298	-7.328790
1873	-36.263293	29.557494	-0.579795	-0.043309	-7.328902
2745	-36.281367	29.575076	-0.579327	-0.043314	-7.328933
4023	-36.290237	29.583798	-0.579005	-0.043317	-7.328761
5858	-36.308459	29.601703	-0.578769	-0.043319	-7.328843
8231	-36.313784	29.606950	-0.578644	-0.043319	-7.328797

is smaller by two orders of magnitude. On the other hand, the orbit-orbit magnetic interaction energies look accurate within one nanohartree. Total relativistic corrections (last column of Table III), calculated with the two largest basis sets, differ by less than $0.1 \mu\text{hartree}$ for all states, although there is no way to extrapolate these results and estimate the error margin more rigorously. For the ground state, the results by Puchalski [18] are available, obtained with the method that

involves regularization of the ∇^4 and $\delta(\mathbf{r})$ operators, which leads to much better convergence, and yields the scalar relativistic correction amounting to -7.515977 mhartree. This means that the error of best present calculation amounts to $0.141 \mu\text{hartree}$.

In order to compare the computed excitation energies with experimental data, nuclear mass proper for a particular isotope has to be taken into account. The most abundant isotopes

TABLE IV. Variationally bound, and extrapolated nonrelativistic energies (in hartree), and scalar relativistic corrections (in mhartree) for ^{11}B and ^{10}B isotopes of boron.

	$^2P_u(^{11}\text{B})$	$^2P_u(^{10}\text{B})$	$^4P_g(^{11}\text{B})$	$^4P_g(^{10}\text{B})$	$^2D_g(^{11}\text{B})$	$^2D_g(^{10}\text{B})$
E_{nr}	-24.652625854	-24.652502219	-24.520826909	-24.520706030	-24.434765075	-24.434644055
E_{extr}	-24.65262669	-24.65250305	-24.52082728	-24.52070640	-24.43476754	-24.43464652
$\langle \hat{H}_1 \rangle$	-36.906350	-36.905605	-36.173742	-36.173014	-36.306284	-36.300219
$\langle \hat{H}_{1n} \rangle$	-6.5×10^{-12}	-8.6×10^{-12}	-6.3×10^{-12}	-8.4×10^{-12}	-6.3×10^{-12}	-8.4×10^{-12}
$\langle \hat{H}_2 \rangle$	30.043429	30.042975	29.500886	29.500440	29.602345	29.596644
$\langle \hat{H}_3 \rangle$	-0.592094	-0.592086	-0.574607	-0.574600	-0.578563	-0.578680
$\langle \hat{H}_4 \rangle$	-0.057750	-0.057743	-0.027879	-0.027873	-0.043248	-0.043241
$\langle \hat{H}_{4n} \rangle$	-0.003040	-0.003342	-0.002961	-0.003255	-0.002977	-0.003273
E_{RS}	-7.515805	-7.515802	-7.278303	-7.278301	-7.328727	-7.328720

TABLE V. Isotopic shifts for term energies (components in hartree, total in cm^{-1}).

K	$E_{nr}(^{10}\text{B}) - E_{nr}(^{11}\text{B})$	$E_{RS}(^{10}\text{B}) - E_{RS}(^{11}\text{B})$	$E_{rel}(^{10}\text{B}) - E_{rel}(^{11}\text{B})$
2P_u			
7456	0.0001236349	3.0×10^{-9}	27.13538
10304	0.0001236348	3.1×10^{-9}	27.13538
4P_g			
3580	0.0001208790	2.2×10^{-9}	26.53036
4672	0.0001208790	2.2×10^{-9}	26.53036
2D_g			
5858	0.0001210195	6.8×10^{-9}	26.56220
8231	0.0001210195	6.9×10^{-9}	26.56222

of boron are ^{11}B and ^{10}B , whose nuclear masses amount to 20 063.7375 a.u. and 18 247.4689 a.u., respectively. The same basis sets are used in the calculations, as for fixed nucleus—only the linear parameters are allowed to vary. Table IV lists the nonrelativistic energies and all components of scalar relativistic corrections, for the largest basis, for each state. Extrapolations to complete basis sets are carried out with the same corrections as for fixed nucleus. Concerning the terms not appearing for fixed nucleus, $\langle \hat{H}_{1n} \rangle$ is damped effectively by the third power of the nuclear mass in the denominator, and amounts to few femtohartree only, which is negligible at the accuracy level achieved in present calculations. On the other hand, $\langle \hat{H}_{4n} \rangle$ amount to few $\mu\text{hartree}$. Other components' values, however, change to such an extent that total scalar relativistic corrections differ from those obtained for fixed nucleus by few nanohartree only.

The wave numbers proper for excitations from the ground state to the lowest 4P_g and 2D_g states, calculated for ^{11}B , and not accounting for the fine structure, amount to $28\,978.75\text{ cm}^{-1}$ and $47\,855.62\text{ cm}^{-1}$, respectively. The latter differs from the experiment-based one by 9 cm^{-1} , which is comparable with the energy difference between the $^2P_{1/2}$ and $^2P_{3/2}$ states (fine structure, 15 cm^{-1}) [3]. Similar accuracy is expected for the excitation energy to the 4P_g state.

The isotopic shifts may be easily calculated from present results. The differences of term energies, between ^{11}B and ^{10}B , computed with the same basis, remain very stable as the basis size is increased—similarly as for the carbon atom [20].

They are given in Table V, with a larger number of significant digits than total energy, for the two largest basis sets. Isotopic shift of -0.57316 cm^{-1} is obtained for the $^2P_u \rightarrow ^2D_g$ excitation, while the measured value, averaged over two spectral lines, is equal to $-0.569(3)\text{ cm}^{-1}$ [28]; -0.60502 cm^{-1} is predicted for the $^2P_u \rightarrow ^4P_g$ transitions.

IV. CONCLUSIONS

The present work provides most accurate to date, nonrelativistic energies of the lowest 2P_u , 4P_g , and 2D_g states of the boron atom. With scalar relativistic corrections and finite nuclear mass taken into account, term energies are obtained, whose main source of remaining error is the missing fine structure. The measured fine splitting amounts to c.a. 15 cm^{-1} for the 2P_u term, c.a. 11 cm^{-1} for the 4P_g term, and less than 1 cm^{-1} for the 2D_g term [3]. The computed $^2P_u \rightarrow ^2D_g$ excitation energy confirms the experiment-based result within c.a. 11 cm^{-1} , and comparable accuracy is expected for the $^2P_u \rightarrow ^4P_g$ excitation. This reveals gross inaccuracy of the latter excitation energy, based on experimental data for heavier, isoelectronic ions. This inaccuracy exceeds 300 cm^{-1} , therefore an update of the content of Atomic Spectra Database [3] would be recommended, concerning the energies of the quartet states of the boron atom. It is worth noting that the predictions of the MCHF study [7] were accurate within 20 cm^{-1} . Further calculations that would include splitting of energy levels due to magnetic spin-orbit and spin-spin couplings are desired.

On the technical side of the work, it is proven again that the symmetrized, explicitly correlated Gaussian lobe functions form an efficient basis for atomic states, in spite of not being eigenfunctions of the \hat{L}^2 operator. Lower variational energies are obtained at shorter expansions, than with basis functions having exact symmetry properties.

ACKNOWLEDGMENTS

This research was supported by Department of Physical and Quantum Chemistry of Wrocław University of Science and Technology. Most calculations have been carried out in Wrocław Center for Networking and Supercomputing (WCSS).

-
- [1] N. Hölsch, M. Beyer, E. J. Salumbides, K. S. E. Eikema, W. Ubachs, C. Jungen, and F. Merkt, *Phys. Rev. Lett.* **122**, 103002 (2019).
- [2] M. Puchalski, J. Komasa, P. Czachorowski, and K. Pachucki, *Phys. Rev. Lett.* **122**, 103003 (2019).
- [3] A. Kramida, Yu. Ralchenko, J. Reader, and *NIST ASD Team* (2019), NIST Atomic Spectra Database (Version 5.7.1) (National Institute of Standards and Technology, Gaithersburg, 2020), available online at <https://physics.nist.gov/asd>.
- [4] A. E. Kramida and A. N. Ryabtsev, *Phys. Scr.* **76**, 544 (2007).
- [5] P. Jönsson and C. Froese Fischer, *Phys. Rev. A* **50**, 3080 (1994).
- [6] F. J. Gálvez, E. Buendía, and A. Sarsa, *J. Chem. Phys.* **122**, 154307 (2005).
- [7] C. Froese Fischer, S. Verdebout, M. Godefroid, P. Rynkun, P. Jönsson, and G. Gaigalas, *Phys. Rev. A* **88**, 062506 (2013).
- [8] C. Chen, *Eur. Phys. J. D* **69**, 128 (2015).
- [9] H. Nakatsuji, H. Nakashima, and Y. I. Kurokawa, *J. Chem. Phys.* **149**, 114106 (2018).
- [10] F. Sasaki and M. Yoshimine, *Phys. Rev. A* **9**, 17 (1974).
- [11] D. Feller and E. R. Davidson, *J. Chem. Phys.* **88**, 7580 (1988).

- [12] H. Meyer, T. Müller, and A. Schweig, *Chem. Phys.* **191**, 213 (1995).
- [13] M. B. Ruiz, in *Advances in the Theory of Quantum Systems in Chemistry and Physics*, Progress in Theoretical Chemistry and Physics, Vol. 22, edited by P. E. Hoggan *et al.* (Springer, Dordrecht, Heidelberg, London, New York, 2012), pp. 103–117.
- [14] R. J. Gdanitz, *J. Chem. Phys.* **109**, 9795 (1998).
- [15] P. Seth, P. L. Rios, and R. J. Needs, *J. Chem. Phys.* **134**, 084105 (2011).
- [16] C. X. Almora-Diaz and C. F. Bunge, *Int. J. Quantum Chem.* **110**, 2982 (2010).
- [17] S. Bubin and L. Adamowicz, *Phys. Rev. A* **83**, 022505 (2011).
- [18] M. Puchalski, J. Komasa, and K. Pachucki, *Phys. Rev. A* **92**, 062501 (2015).
- [19] K. Strasburger, *J. Chem. Phys.* **141**, 044104 (2014).
- [20] K. Strasburger, *Phys. Rev. A* **99**, 052512 (2019); **99**, 069901(E) (2019).
- [21] J. Cioslowski, K. Strasburger, and E. Matito, *J. Chem. Phys.* **136**, 194112 (2012).
- [22] J. Cioslowski, K. Strasburger, and E. Matito, *J. Chem. Phys.* **141**, 044128 (2014).
- [23] J. Cioslowski and K. Strasburger, *J. Chem. Phys.* **148**, 144107 (2018).
- [24] K. Strasburger, *J. Chem. Phys.* **144**, 234304 (2016).
- [25] E. R. Davidson, D. Feller, and P. Phillips, *Chem. Phys. Lett.* **76**, 416 (1980).
- [26] W. Kutzelnigg, *Mol. Phys.* **90**, 909 (1997).
- [27] N. J. A. Sloane, *The Online Encyclopedia of Integer Sequences*, available online at <http://oeis.org/A000930>.
- [28] S. G. Johansson, U. Litzén, J. Kasten, and M. Kock, *Astrophys. J.* **403**, L25 (1993).